

LA-UR-16-21424

Approved for public release; distribution is unlimited.

Title: M-Adapting Low Order Mimetic Finite Differences for Dielectric Interface Problems

Author(s): McGregor, Duncan A.  
Gyrya, Vitaliy  
Manzini, Gianmarco

Intended for: Report

Issued: 2016-03-07

---

**Disclaimer:**

Los Alamos National Laboratory, an affirmative action/equal opportunity employer, is operated by the Los Alamos National Security, LLC for the National Nuclear Security Administration of the U.S. Department of Energy under contract DE-AC52-06NA25396. By approving this article, the publisher recognizes that the U.S. Government retains nonexclusive, royalty-free license to publish or reproduce the published form of this contribution, or to allow others to do so, for U.S. Government purposes. Los Alamos National Laboratory requests that the publisher identify this article as work performed under the auspices of the U.S. Department of Energy. Los Alamos National Laboratory strongly supports academic freedom and a researcher's right to publish; as an institution, however, the Laboratory does not endorse the viewpoint of a publication or guarantee its technical correctness.

# M-Adapting Low Order Mimetic Finite Differences for Dielectric Interface Problems

V. Gyrya, G. Manzini, D. A. McGregor

Summer 2015

## Abstract

We consider a problem of reducing numerical dispersion for electromagnetic wave in the domain with two materials separated by a flat interface in 2D with a factor of two difference in wave speed. The computational mesh in the homogeneous parts of the domain away from the interface consists of square elements. Here the method construction is based on m-adaptation construction in homogeneous domain that leads to fourth-order numerical dispersion (vs. second order in non-optimized method). The size of the elements in two domains also differs by a factor of two, so as to preserve the same value of Courant number in each. Near the interface where two meshes merge the mesh with larger elements consists of degenerate pentagons. We demonstrate that prior to m-adaptation the accuracy of the method falls from second to first due to breaking of symmetry in the mesh. Next we develop m-adaptation framework for the interface region and devise an optimization criteria. We prove that for the interface problem m-adaptation cannot produce increase in method accuracy. This is in contrast to homogeneous medium where m-adaptation can increase accuracy by two orders.

## 1 Introduction

Numerical solution of wave equations in the time domain is a fundamental problem for modeling numerous physical phenomena in heterogeneous media and in domains with complicated geometry that does not allow for a tractable analytical solution. In this report we focused on electromagnetic waves, but all the same difficulties and solution strategies apply to most other wave phenomena (acoustics, elasticity, etc.).

The two main challenges are method accuracy and efficiency. The main contributing factors to the long-time integration error for wave problems is *numerical dispersion* - artificial dependence of the numerical speed of the wave on its frequency, the discretization mesh, and the direction of propagation with respect to the mesh.

There are a number of strategies that are being used in order to reduce the numerical dispersion. Increasing the order of the numerical discretization is one of such strategies. This is a good approach for explicit Finite Difference (FD) schemes, but is rather inefficient for Finite Element (FE) schemes due to the presence of non-diagonal mass matrix in front of the unknown time-step solution. For example, for acoustics when using central difference discretization in time one has to solve the following linear problem at every time step

$$\mathbb{M}U^{n+1} = \mathbb{M}U^{n-1} + \Delta t \mathbb{A}U^n,$$

where  $\mathbb{M}$  is the mass matrix approximating identity and  $\mathbb{A}$  is the stiffness matrix approximating Laplace operator. In FD methods the mass matrix  $\mathbb{M}$  is replaced by identity.

Another strategy that works for rectangular and square meshes is based on forming a parameterized family of methods and optimizing the parameters to improve the dispersion properties. In the FD framework such a family is typically formed by combining several discretizations of the same differential operator (e.g. Laplace operator) that use different stencils. This includes rotated stencils and stencils of larger size. For Maxwell's equation in 3D this approach was taken Smith et.al. in [1]. In the FE framework such a family is obtained using modified quadrature approach. Here one varies the positions of quadrature

points. This changes the approximation error of the integrals (i.e. changes mass and stiffness matrices) for higher order polynomials. This approach for example was taken in [2] for acoustic equation by Yue and Guddati. Mimetic Finite Difference (MFD) methods are relatively new family of methods that share common features with FD and FE methods, see e.g. [3, 4] for the introduction and an overview of these methods. In MFD parameters appear due to flexibility of choosing non-polynomial basis functions. This can be viewed as analogous to the modified quadrature approach in FE discretizations, but not quite the same. The process of adapting free parameters in MFD is dubbed m-adaptation, see e.g. [5] for various applications of m-adaptation. M-adaptation was used for dispersion reduction in acoustics [6, 7] and for electromagnetic equation [8].

M-adaptation showed excellent results on rectangular and square meshes in homogeneous domains, where numerical dispersion was reduced by at least two orders. The next level of difficulty is to consider wave propagation in a domain with two materials separated by a flat interface. For simplicity of presentation suppose a jump in wave speed with a factor of two between the two materials. If one decides to partition the domain using a uniform square mesh the CFL stability condition for these domains then will dictate the largest time step size that is also different by a factor of two. This would mean that in the domain with slower wave speed the numerical scheme is half as efficient as it could be. From the point of view of efficiency when using a uniform time step throughout the domain the best partitioning of the domain would reflect the jump in the wave speed. That is in the part of the domain with faster wave speed one would use mesh that is half the size of that in the slower part of the domain, see Figure 2. FD methods do not have a natural way of discretization for such a mesh. MFD methods for such a mesh, on the other hand, work as well as for a uniform mesh.

The main idea for our work was to consider a mesh with double refinement based on MFD discretization. In principle, the refinement can be by any factor, but double refinement is a good start as a proof of principle. In the homogeneous parts of the domain (away from the interface) we assume use of parameters obtained in [8] using m-adaptation. Around the interface we will try to choose the parameters so as to obtain the method with smallest dispersion error possible.

The report is organized as follows. In Section 2 we present a continuum PDE model to be considered in 2D, its plane wave solution in homogeneous medium and the extension of plane wave to the interface problem which consists of incident, transmitted and reflected waves. In Section 3 we present MFD construction on general meshes and method optimization (m-adaptation) of the method on square meshes for homogeneous medium. In Section 4 we present the problem of dispersion reduction for the interface problem, detailed solution strategy, analysis, and main results. Finally, in Section 5 we present conclusions for our analysis and identify future directions for research.

## 2 Continuum Modelling

We begin by presenting the transverse electric (TE) formulation of Maxwell's equations in 2D. In this formulation one assumes that all functions are constant in  $z$ -direction. This assumption allows to decouple Maxwell's equations into two sets of independent equations in 2D. We will focus on the equations governing the electric induction field,  $\mathbf{D}$ , the current density,  $\mathbf{J}$ , the magnetic field,  $\mathbf{H}$ , the magnetic induction,  $\mathbf{B}$ , the electric field,  $\mathbf{E}$ , and the charge density,  $\rho$ :

$$\begin{aligned} \partial_t \mathbf{D} + \mathbf{J} &= \mathbf{curl} \mathbf{H}, & \text{(Ampere-Maxwell Law)} \\ \partial_t \mathbf{B} &= -\mathbf{curl} \mathbf{E}, & \text{(Faraday's Law)} \\ \nabla \cdot \mathbf{D} &= \rho. & \text{(Gauss' Law)} \end{aligned}$$

The 3D curl operator was replaced by two operators **curl** and curl. The first one is a vector curl, defined as  $\mathbf{curl}f = (\partial_y f, -\partial_x f)^T$ , and the second one is a scalar curl, defined as  $\text{curl}v = \partial_x v_2 - \partial_y v_1$ .

We will assume linear constitutive laws:

$$\mathbf{D} = \epsilon \mathbf{E}, \quad (2.1)$$

$$B = \mu H, \quad (2.2)$$

$$\mathbf{J} = \sigma \mathbf{E} + \mathbf{J}_{\text{ext}}, \quad (2.3)$$

where  $\epsilon$  is the electrical permittivity,  $\mu$  is the magnetic permeability,  $\sigma$  is the electrical conductivity, and  $\mathbf{J}_{\text{ext}}$  an external current density. We will assume that there are constants such that

$$0 < \underline{c} \leq \epsilon, \mu \leq \bar{c} < \infty \quad (2.4)$$

$$0 \leq \sigma \leq \bar{c} < \infty. \quad (2.5)$$

Given that we have three differential equations and three algebraic equations we eliminate variables down to three equations. Our preference is for what we refer to as **E-B** formulation, namely, we eliminate  $\mathbf{D}$  and  $H$  to end up with

$$\partial_t \epsilon \mathbf{E} + \sigma \mathbf{E} = \mathbf{curl} \mu^{-1} B - \mathbf{J}_{\text{EXT}}, \quad (\text{Ampere-Maxwell Law})$$

$$\partial_t B = -\mathbf{curl} \mathbf{E}. \quad (\text{Faraday's Law})$$

$$\nabla \cdot \epsilon \mathbf{E} = \rho \quad (2.6)$$

By taking the divergence of the Ampere-Maxwell law we can derive the Continuity Equation which governs conservation of charge.

$$\nabla \cdot \partial_t \epsilon \mathbf{E} + \nabla \cdot \sigma \mathbf{E} + \nabla \cdot \mathbf{J}_{\text{EXT}} = \nabla \cdot \mathbf{curl} \mu^{-1} B \quad (2.7)$$

$$\partial_t \rho = -\nabla \cdot (\sigma \mathbf{E} + \mathbf{J}_{\text{EXT}}) \quad (2.8)$$

The continuity equation informs us that the divergence of  $\mathbf{E}$  is governed by its initial conditions, the presence of external sources, and the conductivity of the media. In a source free domain without conductivity we would expect that  $\nabla \cdot \mathbf{E} = 0$  for all time assuming that at time zero the field was divergence free.

## 2.1 Plane Wave Solutions

For source free (i.e.  $\mathbf{J}_{\text{EXT}} \equiv 0$ ) Cauchy problems we can construct plane-wave solutions to Maxwell's Equations. Even on bounded domains, planewaves are dense in the solution space of Maxwell's equations. We will now proceed with a classical dispersion analysis and then perform mode-matching to generate plane-wave solutions at a simple dielectric interface. Suppose that  $(\epsilon, \mu, \sigma)$  are constant on  $\mathbb{R}^2$ . Then we can construct a plane-wave solution to the system using the dispersion relationship derived by assuming the solution of the form

$$\mathbf{E} = \mathbf{E}_0 \exp i(\mathbf{k} \cdot \mathbf{x} - \omega t) \quad (2.9)$$

$$B = B_0 \exp i(\mathbf{k} \cdot \mathbf{x} - \omega t). \quad (2.10)$$

This can then be substituted into the equation to produce the following system of equations

$$(-i\omega\epsilon + \sigma) \mathbf{E}_0 = i\mu^{-1} \mathbf{k} \times B_0 \quad (2.11)$$

$$-i\omega B_0 = i\mathbf{k} \times \mathbf{E}_0 \quad (2.12)$$

We can then eliminate the  $B_0$  and this will produce the following dispersion relationship

$$\left( -\omega^2 - i\omega \frac{\sigma}{\epsilon} \right) \mathbf{E}_0 = c^2 \mathbf{k} \times \mathbf{k} \times \mathbf{E}_0 \quad (2.13)$$

This leads to an 2x2 eigenvalue problem. Note that the matrix which encodes  $\mathbf{k} \times \mathbf{k} \times$  has eigenvectors  $\mathbf{k}^\perp$  and  $\mathbf{k}$  and respective eigenvalues  $-\mathbf{k}^2$  and 0. The  $\mathbf{k}^\perp$  component will obey the relationship

$$-\omega^2 - i\frac{\sigma}{\epsilon}\omega = -c^2|\mathbf{k}|^2 \quad (2.14)$$

$$\omega = -i\frac{\sigma}{2\epsilon} \pm \sqrt{c^2|\mathbf{k}|^2 - \frac{\sigma^2}{4\epsilon^2}} \quad (2.15)$$

$$\mathbf{E} = \mathbf{k}^\perp \exp \left( i\mathbf{k} \cdot \mathbf{x} - t \left( \frac{\sigma}{2\epsilon} \pm i\sqrt{c^2|\mathbf{k}|^2 - \frac{\sigma^2}{4\epsilon^2}} \right) \right) \quad (2.16)$$

To determine  $B_0$  then solve using Equation (2.12) and (2.16).

$$B = \frac{|\mathbf{k}|^2}{\omega} \exp \left( i\mathbf{k} \cdot \mathbf{x} - t \left( \frac{\sigma}{2\epsilon} \pm i\sqrt{c^2|\mathbf{k}|^2 - \frac{\sigma^2}{4\epsilon^2}} \right) \right). \quad (2.17)$$

Now considering the  $\mathbf{k}$  eigenvalue we are left with the following algebraic system.

$$-\omega \left( \omega + i\frac{\sigma}{\epsilon} \right) = 0 \quad (2.18)$$

$$\omega = -i\frac{\sigma}{\epsilon} \quad \omega = 0 \quad (2.19)$$

We will neglect the case  $\omega = 0$  as the continuity equation is consistent with  $\omega = -i\frac{\sigma}{\epsilon}$ . In the case  $\sigma = 0$  we have that the  $\mathbf{k}$  mode will be forced to zero (i.e. the planewave will be divergence zero). In the more general case there are two classes of waves transient, decaying waves and evanescent (stationary, decaying) waves.

$$\mathbf{E} = \mathbf{k} \exp \left( i\mathbf{k} \cdot \mathbf{x} - \frac{\sigma}{\epsilon}t \right) \quad \mathbf{B} \equiv 0 \quad (2.20)$$

We will neglect the case  $\omega = 0$  as the continuity equation is consistent with  $\omega = -i\frac{\sigma}{\epsilon}$ . In the case  $\sigma = 0$  we have that the  $\mathbf{k}$  mode will be forced to zero (i.e. the planewave will be divergence zero). In the more general case there are two classes of waves transient, decaying waves and evanescent (stationary, decaying) waves.

We will begin with a simple interface problem. Let  $G_1$  be the upper half plane,  $G_2$  be the lower half plane, and  $\Gamma$  be the real line. Let

$$\epsilon(x, y) = \begin{cases} \epsilon_1 & y > 0 \\ \epsilon_2 & y < 0 \end{cases} \quad (2.21)$$

$$\mu(x, y) = \begin{cases} \mu_1 & y > 0 \\ \mu_2 & y < 0 \end{cases} \quad (2.22)$$

$$\sigma = 0 \quad (2.23)$$

We know that we can construct solutions to Maxwell's equations in the top and bottom half planes respectively. One technique to compute a global solution is to take linear combinations of solutions on each subdomain and then try and satisfy some interface condition. Interface conditions for Maxwell's equations are well known and can be derived from the integral formulation of the system, c.f. [9]. Let  $\boldsymbol{\tau}$  be the unit-tangent vector to  $\Gamma$  and  $\mathbf{n}$  be the unit normal vector to  $\Gamma$ .

$$(\mathbf{E}|_{G_1} - \mathbf{E}|_{G_2}) \cdot \boldsymbol{\tau} = 0 \quad (2.24)$$

$$((\epsilon\mathbf{E})|_{G_1} - (\epsilon\mathbf{E})|_{G_2}) \cdot \mathbf{n} = 0 \quad (2.25)$$

$$((\mu^{-1}B)|_{G_1} - (\mu^{-1}B)|_{G_2}) = 0 \quad (2.26)$$

See Figure 1 for an illustration of our problem of interest. A solution to the mode matching can be found

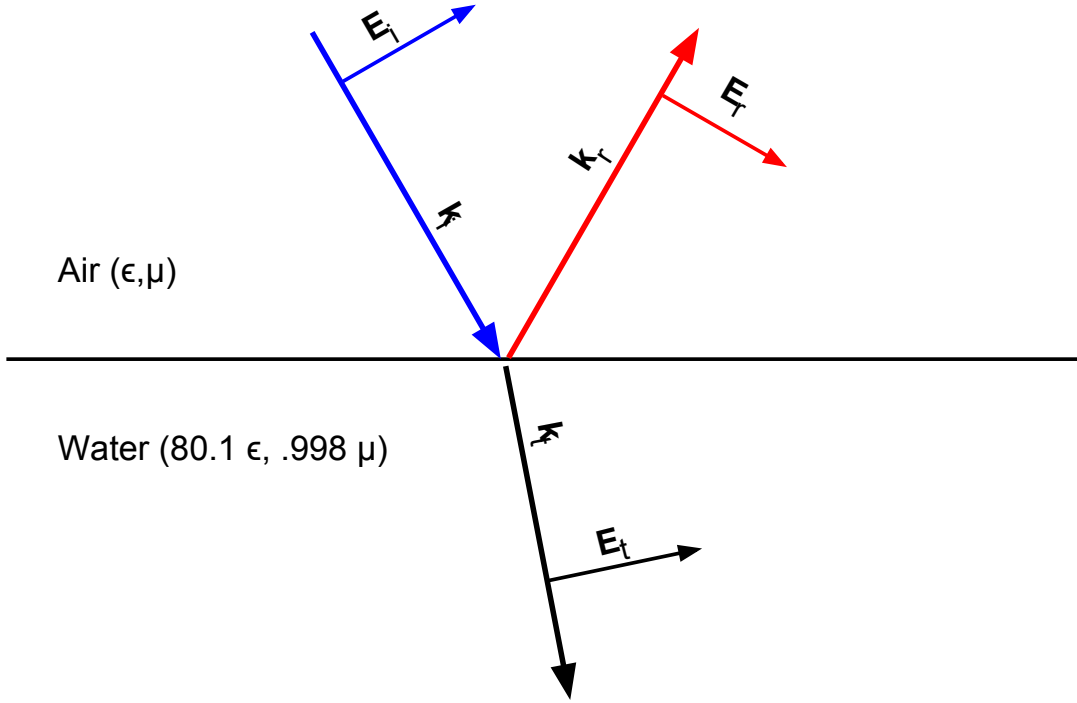


Figure 1: Simple transmission at an air-water interface

using the following Ansatz:

$$\mathbf{E}(\mathbf{x}, t) = \begin{cases} \widetilde{\mathbf{E}}_i \exp i(\mathbf{k}_i \cdot \mathbf{x} - \omega t) + \widetilde{\mathbf{E}}_r \exp i(\mathbf{k}_r \cdot \mathbf{x} - \omega t) & \in G_1 \times T, \\ \widetilde{\mathbf{E}}_t \exp i(\mathbf{k}_t \cdot \mathbf{x} - \omega t) & \in G_2 \times T, \end{cases} \quad (2.27)$$

$$\mathbf{k}_i = k_i(-\sin \theta_i, \cos \theta_i)^T \quad \mathbf{k}_t = k_t(-\sin \theta_t, \cos \theta_t)^T \quad \mathbf{k}_r = k_r(-\sin \theta_r, \cos \theta_r)^T, \quad (2.28)$$

$$\widetilde{\mathbf{E}}_i = \mathbf{k}_i^\perp \quad \widetilde{\mathbf{E}}_t = E_t \mathbf{k}_t^\perp \quad \widetilde{\mathbf{E}}_r = E_r \mathbf{k}_r^\perp. \quad (2.29)$$

Repeating the classical exercise, c.f. [9], we can write  $E_r, E_t, k_r, k_t, \theta_r, \theta_t$  as functions of the incident variables.

$$k_i = k_r = \omega \sqrt{\epsilon_1 \mu_1} \quad k_r = \omega \sqrt{\epsilon_2 \mu_2} \quad (2.30)$$

$$\mathbf{k}_r = k_i(-\sin \theta_i, -\cos \theta_i)^T \quad (2.31)$$

$$\sin \theta_t = \frac{\epsilon_1 \mu_1}{\epsilon_2 \mu_2} \sin \theta_i \quad (2.32)$$

$$(2.33)$$

To determine the quantities  $E_t, E_r$  we have to introduce additional quantities.

$$\alpha = \frac{\cos \theta_t}{\cos \theta_i} \quad (2.34)$$

$$\beta = \frac{\epsilon_2}{\epsilon_1} \quad (2.35)$$

$$E_r = \frac{\alpha - \beta}{\alpha + \beta} E_i \quad (2.36)$$

$$E_t = \frac{2}{\alpha + \beta} E_i \quad (2.37)$$

### 3 Low Order Mimetic Finite Differences

The mimetic finite difference method has seen development for a long time particularly for electromagnetic applications, c.f. [3]. In this section we will present the modern theory of the method found in [10] and apply it to our specific problem.

Let  $G$  be our computational domain and  $\mathcal{T}$  be a mesh on  $G$  with edges  $\mathcal{E}$  and cells (or faces)  $\mathcal{F}$ . We will consider a Mimetic discretization where  $\mathbf{E} \approx \mathbf{E}_h \in \mathcal{E}_h$  and  $B \approx B_h \in \mathcal{F}_h$ . These discrete spaces are defined by their interpolants and their domains.

$$\mathcal{I}^{\mathcal{E}_h} : \mathbf{H}(\text{curl}, G) \rightarrow \mathcal{E}_h \quad (3.1)$$

$$\mathcal{I}^{\mathcal{E}_h}(\mathbf{E}) = \left( \frac{1}{|e|} \int_e \mathbf{E} \cdot \boldsymbol{\tau} de, e \in \mathcal{E} \right) \quad (3.2)$$

$$\mathcal{I}^{\mathcal{F}_h} : L^2 \rightarrow \mathcal{F}_h \quad (3.3)$$

$$\mathcal{I}^{\mathcal{F}_h}(B) = \left( \frac{1}{|f|} \int_f B df, f \in \mathcal{F} \right) \quad (3.4)$$

To denote the restriction of the interpolant to a structure (e.g.  $e \in \mathcal{E}$  or  $f \in \mathcal{F}$ ) we use an appropriate subscript. We define a discrete scalar curl called  $\text{curl}_h$  by the commutativity relationships

$$\text{curl}_h \circ \mathcal{I}^{\mathcal{E}_h} = \mathcal{I}^{\mathcal{F}_h} \circ \text{curl}. \quad (3.5)$$

We therefore will calculate  $\mathcal{I}_f^{\mathcal{F}_h}(\text{curl}\mathbf{E})$  and rewrite it as a linear combination of the degrees of freedom of  $\mathcal{I}_f^{\mathcal{E}_h}$ .

$$\mathcal{I}_f^{\mathcal{F}_h}(\text{curl}\mathbf{E}) = \frac{1}{|f|} \int_f \text{curl}\mathbf{E} df = \frac{1}{|f|} \sum_{e \in \partial f} \int_e \boldsymbol{\tau} \cdot \mathbf{E} de \quad (3.6)$$

$$= \frac{1}{|f|} \sum_{e \in \partial f} \sigma_{e,f} |e| \mathcal{I}_e^{\mathcal{E}_h}(\mathbf{E}) \quad (3.7)$$

Here  $\sigma_{e,f} = \pm 1$  is an orientation vector which corrects for the possible discrepancy in the global orientation of edges and the necessary counter-clockwise orientation of the circulation integral.

Our inner product matrices will satisfy the following

$$\mathcal{I}_f^{\mathcal{E}_h}(\mathbf{E})^T \mathbb{M}_{\mathcal{E}|f} \mathcal{I}_f^{\mathcal{E}_h}(\mathbf{D}) = \int_f \mathbf{E} \cdot \mathbf{D} + \mathcal{O}(h) \quad (3.8)$$

$$\mathcal{I}_f^{\mathcal{F}_h}(B)^T \mathbb{M}_{\mathcal{F}|f} \mathcal{I}_f^{\mathcal{F}_h}(C) = \int_f BC + \mathcal{O}(h) \quad (3.9)$$

The inner product matrices  $\mathbb{M}_{\mathcal{S}}$  are constructed locally and we use the notation that the local matrix restricted to a grid cell  $f$  is given denoted  $\mathbb{M}_{\mathcal{S},f}$ . We use similar notation for the local degrees of freedom and differential operators. Given that our degrees of freedom for  $\mathcal{F}$  functions are average values, the local construction is straight forward.

$$\mathbb{M}_{\mathcal{F},f}^{\mu^{-1}} B_{h,Q} = |f| \overline{\mu^{-1}} B_{h,f} \quad \overline{\mu^{-1}} = \frac{1}{|f|} \int_f \mu^{-1} \quad (3.10)$$

The above description implies that  $\mathbb{M}_{\mathcal{F},f} = |f| \overline{\mu^{-1}}$ . This approximation is order  $h$  accurate which suffices. To construct the edge based we rely on a so called polynomial consistency condition.

**Definition 3.1.** Let  $\mathbb{M}$  be a mass matrix restricted to a local cell  $P$ . Then  $\mathbb{M}$  obeys polynomial consistency if there exist matrices  $\mathbb{N}$  and  $\mathbb{R}$  such that

- $MN = \mathbb{R}$
- $N^T \mathbb{R}$  is symmetric positive definite.

**Lemma 3.1.** Let  $N \in \mathbf{R}^{n \times m}$  be rank  $m$ ,  $\text{Im}(\mathbb{Q}) = \text{Ker}(\mathbb{R}^T)$ , and let  $N^T \mathbb{R}$  be symmetric positive definite.

$$M = \mathbb{R}(N^T \mathbb{R})^{-1} \mathbb{R}^T + \mathbb{P} \quad (3.11)$$

$$\mathbb{P} = \mathbb{Q} \mathbb{C} \mathbb{Q}^T \quad (3.12)$$

then

1.  $MN = \mathbb{R}$
2.  $\text{Im}(N) = \text{Im}(\mathbb{R})$
3. if  $\mathbb{C}$  is spd then  $M$  is spd.

*Proof.* The proof of (1) is an immediate calculation.

$$\mathbb{R}(N^T \mathbb{R})^{-1} \mathbb{R}^T N = \mathbb{R} \quad N^T \mathbb{R} \text{ symmetric} \quad (3.13)$$

$$\mathbb{Q} \mathbb{C} \mathbb{Q}^T N = \mathbf{0} \quad \mathbb{Q}^T N = \mathbf{0} \quad (3.14)$$

We will now prove (2). Note that  $\mathbf{R}^n = \text{Im}(N) \oplus \text{Im}(\mathbb{Q})$ . Assume that  $\mathbf{x} \in \text{Ker}(\mathbb{R})$  is non-zero. As  $\mathbb{R}^T N$  is spd we know that  $\mathbf{x} = \mathbb{Q}\mathbf{y}$ .

$$\therefore \text{Ker}(\mathbb{R}^T) \subset \text{Im}(\mathbb{Q}) \quad (3.15)$$

$$\therefore (\text{Im}(\mathbb{R}))^\perp \subset \text{Im}(\mathbb{Q}) \quad \text{Closed Range Theorem} \quad (3.16)$$

$$\therefore (\text{Im}(\mathbb{R}))^\perp \subset (\text{Im}(N))^\perp \quad \text{By Assumption} \quad (3.17)$$

However as  $N^T \mathbb{R}$  is spd we have that  $\mathbb{R}$  and  $N$  are of the same rank therefore the dimension of their orthogonal complements must be the same. Pidgeon hole principle therefore implies the following.

$$(\text{Im}(\mathbb{R}))^\perp = (\text{Im}(N))^\perp \implies \text{Im}(\mathbb{R}) = \text{Im}(N) \quad (3.18)$$

We will now show (3). Let  $\mathbb{C}$  be spd. Then symmetry and non-negativity of  $M$  are immediate. Let  $\mathbf{z} = N\mathbf{x} + \mathbb{Q}\mathbf{y}$ .

$$\mathbf{z}^T M \mathbf{z} = (\mathbb{R}^T \mathbf{z})^T (N^T \mathbb{R})^{-1} (\mathbb{R}^T \mathbf{z}) + (\mathbb{Q}^T \mathbf{z})^T \mathbb{C} (\mathbb{Q}^T \mathbf{z}) \quad (3.19)$$

$$= (\mathbb{R}^T N \mathbf{x})^T (N^T \mathbb{R})^{-1} (\mathbb{R}^T N \mathbf{x}) + (\mathbb{Q}^T \mathbb{Q} \mathbf{y})^T \mathbb{C} (\mathbb{Q}^T \mathbb{Q} \mathbf{y}) \quad (3.20)$$

$$= \mathbf{x}^T (N^T \mathbb{R}) \mathbf{x} + \mathbf{y}^T (\mathbb{Q}^T \mathbb{Q})^T \mathbb{C} (\mathbb{Q}^T \mathbb{Q}) \mathbf{y} \quad (3.21)$$

Note that  $\mathbf{q} = \mathbb{Q}^T \mathbb{Q} \mathbf{y} = \mathbf{0}$  if and only if  $\mathbf{y} = \mathbf{0}$  as  $\mathbb{Q}$  is full rank, and  $\text{Im}(\mathbb{Q}) \perp \text{Ker}(\mathbb{Q}^T)$ . Therefore

$$\mathbf{y}^T (\mathbb{Q}^T \mathbb{Q})^T \mathbb{C} (\mathbb{Q}^T \mathbb{Q}) \mathbf{y} = 0 \iff \mathbf{y} = \mathbf{0} \quad (3.22)$$

$$\mathbf{x}^T (N^T \mathbb{R})^{-1} \mathbf{x} = 0 \iff \mathbf{x} = \mathbf{0} \quad (3.23)$$

**Q.E.D.**

To make use of the theorem, one must determine appropriate, computable, forms of the matrix  $N$  and  $\mathbb{R}$ . We choose to pick the values of  $N$  and  $\mathbb{R}$  through consistency relationships. To determine  $N$ , we rely upon a matrix of the degrees of freedom of the standard unit vectors  $\mathbf{e}_1, \mathbf{e}_2$  as they form the basis of  $P_0$ .

$$N_{i,j} = \left( \frac{1}{|e_i|} \int_{e_i} \mathbf{e}_j \cdot \boldsymbol{\tau} : e_i \in \partial f \right). \quad (3.24)$$

Let  $(x_c, y_c)$  be the barycenter of  $f$ . We know that  $\mathbb{M}$  will encode integration against another, arbitrary, grid function we know that  $\mathbb{R}$  must be determined by the following integral

$$\mathbf{e}_1 = \mathbf{curl} (y - y_c) := \mathbf{curl} p_1 \quad \mathbf{e}_2 = \mathbf{curl}(-x + x_c) := \mathbf{curl} p_2 \quad (3.25)$$

$$\int_f \epsilon \mathbf{E} \cdot \mathbf{e}_i \, d\mathbf{x} = \int_f \epsilon \mathbf{E} \cdot \mathbf{curl} p_i \, d\mathbf{x} \quad (3.26)$$

$$= \int_f (\mathbf{curl} \epsilon \mathbf{E}) p_i \, d\mathbf{x} - \sum_{e \in \partial f} \int_e \epsilon \mathbf{E} \cdot \boldsymbol{\tau} p_i \, ds \quad (3.27)$$

To resolve the above integrals, we must introduce an approximation. Namely we will neglect the area integral as it  $\mathcal{O}(h)$  and we will approximate the edge integrals as follows. Let  $d_e$  be the degree of freedom associate with an edge. Let  $\mathbf{x}_e$  be the midpoint of an edge  $e$ .

$$\int_f \epsilon \mathbf{E} \cdot \mathbf{e}_i = - \sum_{e \in \partial f} |e| s_e \epsilon(\mathbf{x}_e) d_e(\mathbf{E}) p_i(\mathbf{x}_e) + \mathcal{O}(h) \quad (3.28)$$

Here  $s_e$  is the orientation scalar as defined in the operator  $\mathbf{curl}_h$ . We define the matrix  $\mathbb{R}$  as follows

$$\mathbb{R}_{i,j} = \frac{1}{|f|} \left( |e_j| s_{e_j} \epsilon(\mathbf{x}_{e_j}) p_i(\mathbf{x}_{e_j}) : e_j \in \partial f \right). \quad (3.29)$$

We will now show the spd property.

$$\mathbb{N}_i^T \mathbb{R}_j = \int_f \mathbf{e}_i \cdot \mathbf{e}_j = |f| \delta_{ij} \quad (3.30)$$

which is obviously symmetric positive definite.

Given this approach, we can construct the edge-based mass matrix. While one could compute using the inverse of appropraite mass matrices using standard techniques, for example using conjugate gradients, we will instead use a non-standard mass lumping technique. Namely we wish to create an approximate inverse matrix which satisfies

$$\mathbb{W} \mathbb{R} = \mathbb{N} \quad (3.31)$$

using the above theorem we can then construct  $\mathbb{W}$  by

$$\mathbb{W} = \mathbb{N} (\mathbb{N}^T \mathbb{R})^{-1} \mathbb{N}^T + \mathbb{Q} \mathbb{U} \mathbb{Q}^T \quad (3.32)$$

Note that the  $\mathbb{Q}$  available in this construction can be selected to be the same matrix as in the  $\mathbb{M}$  construction by the preceeding Lemma, namely as  $\text{Im}(\mathbb{R}) = \text{Im}(\mathbb{N})$ . Note the following:

$$\mathbb{W} \mathbb{M} \mathbb{N} = \mathbb{W} \mathbb{R} = \mathbb{N} \quad (3.33)$$

$$\mathbb{M} \mathbb{W} \mathbb{R} = \mathbb{M} \mathbb{N} = \mathbb{R} \quad (3.34)$$

### 3.1 Fully-Discrete Scheme

We will now present two full discrete schemes. We use MFD in space and staggered-leap frog in time. The first scheme when electrical conductivity is not neglected.

$$\mathbf{E}_h^{n+1} = \mathbb{W}_{\mathcal{E}}^{\epsilon + \Delta t \sigma} \left( \mathbb{M}_{\mathcal{E}}^{\epsilon - \Delta t \sigma} \mathbf{E}_h^n + \Delta t \mathbf{curl}_h^T \mathbb{M}_{\mathcal{F}}^{\mu^{-1}} B_h^{n+1/2} \right) \quad (3.35)$$

$$B_h^{n+3/2} = B_h^{n+1/2} - \Delta t \mathbf{curl}_h \mathbf{E}_h^{n+1} \quad (3.36)$$

In the case of negligible conductivity the scheme will be simpler.

$$\mathbf{E}_h^{n+1} = \mathbf{E}_h^n + \Delta t \mathbb{W}_{\mathcal{E}}^\epsilon \operatorname{curl}_h^T \mathbb{M}_{\mathcal{F}}^{\mu^{-1}} B_h^{n+1/2} \quad (3.37)$$

$$B^{n+3/2} = B^{n+1/2} - \Delta t \operatorname{curl}_h \mathbf{E}^{n+1} \quad (3.38)$$

Regardless of the case we will use the notation to denote each time step

$$\mathbf{E}_h^{n+1} = \mathbb{S}_1(\mathbf{E}_h^n, B_h^{n+1/2}) \quad (3.39)$$

$$B^{n+3/2} = \mathbb{S}_2(\mathbf{E}_h^{n+1}, B_h^{n+1/2}) \quad (3.40)$$

### 3.2 M-Adaptation

M-adaptation is the process of picking the matrix  $\mathbb{C}$  or  $\mathbb{U}$  in the definition of our inner product or approximate inner product inverse matrices to optimize the scheme for some objective. In our case we will be picking  $\mathbb{U}$  to attempt to minimize the numerical dispersion of our discrete scheme.

The general idea is to pick a criteria to minimize, like the difference between numerical frequency and physical frequency and expand in a Taylor series. One then picks terms to eliminate terms of this series. In some circumstances though, this approach is not tractable. Instead we can reduce the local truncation error of a plane-wave ansatz after a time timestep.

This technique has been applied in [8] to reduce the dispersion error for Maxwell's equations in uniform media. Namely by choosing the local stabilization matrix

$$\mathbb{P}|_f = \frac{|f|}{12} \begin{pmatrix} 1 & 0 \\ 0 & 1 \\ -1 & 0 \\ 0 & -1 \end{pmatrix} \begin{pmatrix} 4 - \nu^2 & -\nu^2 \\ -\nu^2 & 4 - \nu^2 \end{pmatrix} \begin{pmatrix} 1 & 0 & -1 & 0 \\ 0 & 1 & 0 & -1 \end{pmatrix} \quad (3.41)$$

where  $\nu = \frac{c\Delta t}{h}$  is the Courant number. This choice eliminates the second order dispersion error so that

$$\omega_n^2 = c^2 k^2 + \mathcal{O}(kh)^4 \quad (3.42)$$

where  $\omega_n$  is the numerical frequency and  $k$  is the physical wave number.

For our interface problem we will assume above stabilization matrix in the uniform regions. Our goal will be to produce stabilization matrices which reduce dispersion accross the material discontinuity.

## 4 Discrete Dielectric Interface Problem

Our representative problem is given as follows. Assume a global domain  $G$  which is subdivided into  $G_t$  and  $G_b$ . Will discretize with uniform, square cells in both domains but  $G_b$  will be twice as refined as  $G_t$ . There will be different dielectric properties in each subdomain,  $(\epsilon_t, \mu_t)$ , and  $(\epsilon_b, \mu_b)$ . For an air/water interface we would have  $\epsilon_b > \epsilon_t$  (for example at 20° C,  $\epsilon_b = 81\epsilon_0$  while  $\epsilon_t \approx \epsilon_0$ ) and  $\mu_b \approx \mu_t$ . Let  $c_t = (\epsilon_t \mu_t)^{1/2}$ ,  $c_b = (\epsilon_b \mu_b)^{-1}$ . The difference in material properties will lead to slower propagation in the  $G_b$  with a contraction in wavelength by a factor of  $\frac{c_b}{c_t}$ . For the purpose of the following analysis we will assume that  $c_b = \frac{1}{2}c_t$ .

In Figure 2 we describe degrees of freedom necessary for a single step at several degrees of freedom. For our purposes we will refer to degrees of freedom as  $E_i^y, E_j^x$ , and  $B_\ell$  for  $i, j, \ell$  integers appearing in the figure. Initial values are given as follows

The exact solution is given as follows with  $\alpha_t, \alpha_r$  defined as above. There is some naive non-dimensionalization in place here, namely we have divided by a reference electric field  $|\mathbf{E}_{\text{ref}}|$  (for example by  $\frac{\text{V}}{\text{m}}$ ).

$$E_i^y(x, y, t) = \begin{cases} k_x \exp i(k_x x + k_y^i y - \omega t) + \alpha_r k_x \exp i(k_x x - k_y^i y - \omega t) & y \geq 0 \\ \alpha_t k_x \exp i(k_x + k_y^t y - \omega t) & y < 0 \end{cases} \quad (4.1)$$

$$E_i^x(x, y, t) = \begin{cases} -k_y^i \exp i(k_x x + k_y^i y - \omega t) + \alpha_r k_y^i \exp i(k_x x - k_y^i y - \omega t) & y \geq 0 \\ -k_y^t \exp i(k_x x + k_y^t y - \omega t) & y < 0 \end{cases} \quad (4.2)$$

$$B(x, y, t) = \begin{cases} \frac{|\mathbf{k}^i|^2}{\omega} \left( \exp i(k_x x + k_y^i y - \omega t) + \alpha_r \exp i(k_x x - k_y^i y - \omega t) \right) & y \geq 0 \\ \alpha_t \frac{|\mathbf{k}^t|^2}{\omega} \exp i(k_x x + k_y^t y - \omega t) & y < 0 \end{cases} \quad (4.3)$$

We will consider a special mesh where for  $y > 0$  we will have a uniform Cartesian mesh with side-length  $h$  and for  $y < 0$  we will have uniform Cartesian mesh with side length  $h/2$ . At  $y = 0$  we will have all the degrees of freedom associated with the bottom mesh. For our purposes we will split edges  $e \in \mathcal{E}_h$  into vertical edge  $v$  and horizontal edges  $r$ . While this decomposition is meaningless on a truly general mesh, yet is standard practice in the Yee-scheme. Further, instead of exactly calculating integrals along edges, we will use the midpoint quadrature on every edge and on every cell center.

Further we introduce simplifying constants which reduce the total number of parameters necessary to describe a given initial condition.

$$k_x = k_x^i \quad k_y = k_y^i \quad (4.4)$$

$$c_0 = (\epsilon_1 \mu_1)^{-1/2} \quad \epsilon_0 = \epsilon_2 \epsilon_1^{-1} \quad (4.5)$$

$$\mu_0 = \mu_2 \mu_1^{-1} \quad k = \sqrt{k_x^2 + k_y^2} \quad (4.6)$$

$$k_x = k \cos \theta \quad k_y = k \sin \theta \quad (4.7)$$

$$k_y^T = k \sqrt{(\epsilon_0 \mu_0 - 1) \cos^2 \theta + \sin^2 \theta} \quad \omega = c_0 k \quad (4.8)$$

$$\alpha_r = \frac{\sqrt{1 + (1 - \epsilon_0^{-1} \mu_0^{-1}) \cot^2 \theta} - \epsilon_0^{-1/2} \mu_0^{-3/2}}{\sqrt{1 + (1 - \epsilon_0^{-1} \mu_0^{-1}) \cot^2 \theta} + \epsilon_0^{-1/2} \mu_0^{-3/2}} \quad (4.9)$$

$$\alpha_t = \frac{2}{\sqrt{1 + (1 - \epsilon_0^{-1} \mu_0^{-1}) \cot^2 \theta} + \epsilon_0^{-1/2} \mu_0^{-3/2}} \quad (4.10)$$

Given the Ansatz, it is clear that in the entire domain our solution has the property that if a degree of freedom  $d_i$  is located at position  $(x, y)$  and degree of freedom  $d_j$  is at  $(x + h, y)$ , then  $d_j = \exp(i k_x h) d_i$ . Further we will assume that for cells not adjacent to the interface have their choice of parameters determined by the homogeneous M-adaptation. Namely the local stabilization matrix is chosen as

$$\mathbb{P}|_f = \frac{|f|}{12} \begin{pmatrix} 1 & 0 \\ 0 & 1 \\ -1 & 0 \\ 0 & -1 \end{pmatrix} \begin{pmatrix} 4 - \nu^2 & -\nu^2 \\ -\nu^2 & 4 - \nu^2 \end{pmatrix} \begin{pmatrix} 1 & 0 & -1 & 0 \\ 0 & 1 & 0 & -1 \end{pmatrix} \quad (4.11)$$

where the  $\nu$  is the Courant number,  $\nu = \frac{\Delta t c_t}{h}$ . There are eight degrees of freedom which determine the value of the discrete plane wave at all degrees of freedom. Refer to Figure for numbering, but of interest are edges  $r_7, r_{13}, r_{14}, r_{19}, r_{20}, h_9, h_{14}$ , and  $h_{15}$ . To compute the discrete wave after a time step from exact data, we must also compute  $\mathbb{S}_2(B_h^{-1/2}, \mathbf{E}_h^0)$  and  $\text{curl}_h^T \mathbb{S}_2(B_h^{-1/2}, \mathbf{E}_h^0)$  at all degrees of freedom

However, for those cells adjacent to the interface we have two stabilization matrices which we will work with. We differentiate between the five-edged, coarse grid cells and the four edged, fine grid cells by the

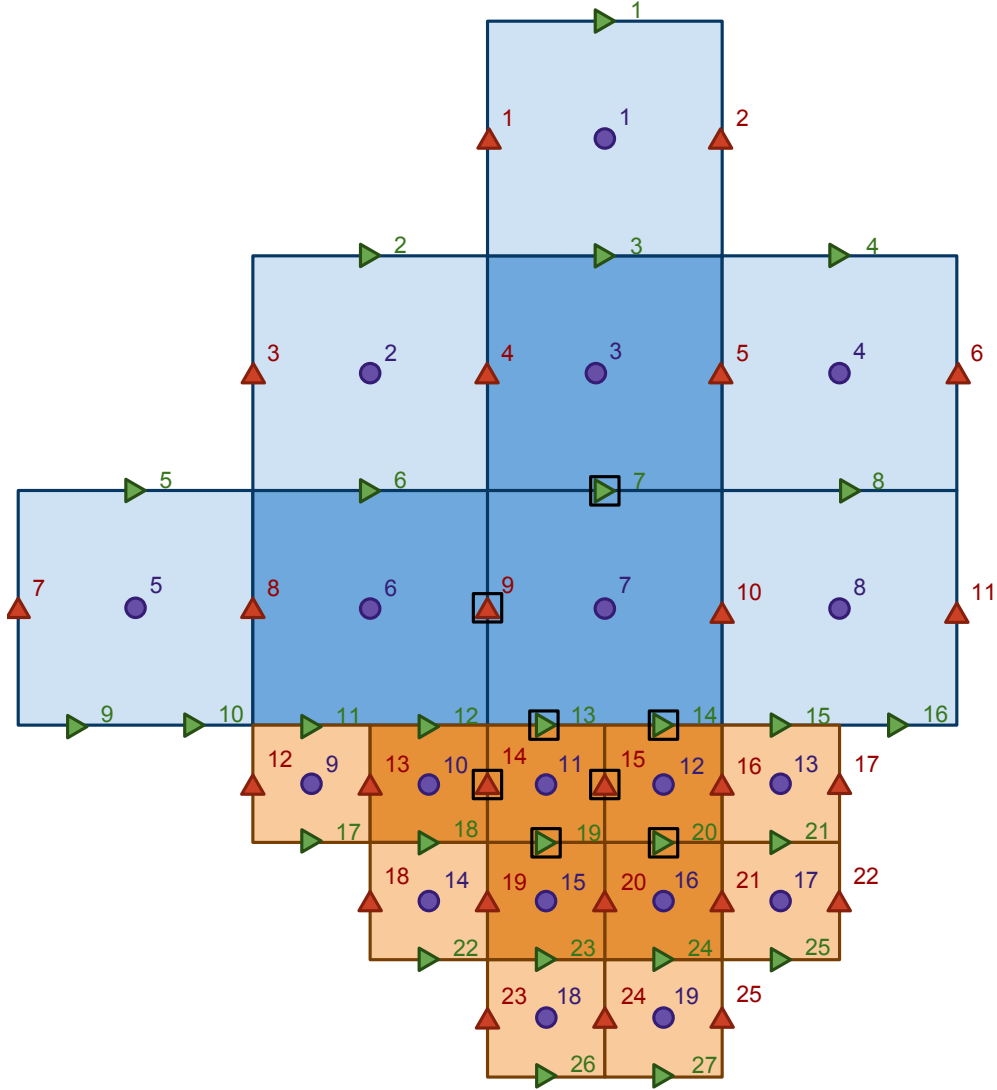


Figure 2: Boxed degrees of freedom represent unique values up to translation by  $(h, 0)$ . We must multiply by the mass matrix in the darker shaded cells. Lighter shaded cells are needed only to form the  $\text{curl}_h^T$ .

subscript 5 and 4 respectively.

$$\mathbb{P}^5 = |f| \begin{pmatrix} 1 & 1 & 0 \\ -1 & 0 & 0 \\ 0 & 0 & 1 \\ 0 & -1 & 0 \\ 0 & 0 & -1 \end{pmatrix} \begin{pmatrix} q_1 & q_2 & q_3 \\ q_2 & q_4 & q_5 \\ q_3 & q_5 & q_6 \end{pmatrix} \begin{pmatrix} 1 & -1 & 0 & 0 & 0 \\ 1 & 0 & 0 & -1 & 0 \\ 0 & 0 & 1 & 0 & -1 \end{pmatrix} \quad (4.12)$$

$$\mathbb{P}^4 = |f| \begin{pmatrix} 1 & 0 \\ 0 & 1 \\ -1 & 0 \\ 0 & -1 \end{pmatrix} \begin{pmatrix} m_1 & m_2 \\ m_2 & m_3 \end{pmatrix} \begin{pmatrix} 1 & 0 & -1 & 0 \\ 0 & 1 & 0 & -1 \end{pmatrix} \quad (4.13)$$

With our matrices constructed we interpolate the Ansatz on our stencil and calculate

$$\mathbb{S}_1(\mathbb{S}_2(B_h^{-1/2}, \mathbf{E}_h^0), \mathbf{E}_h^0)|_e - \mathbf{E}(\cdot, \Delta t)|_e := \text{RES}_e \quad (4.14)$$

where the subscript  $e$  denotes a particular edge. It is the goal to produce a residual at all  $r_7, r_{13}, r_{14}, r_{19}, r_{20}, v_9, v_{14}$ , and  $v_{15}$  with

$$\text{RES}_e = \mathcal{O}(h^2) \quad (4.15)$$

**Theorem 4.1.** *There is no choice of parameters independent of  $k$  and  $\theta$  for which  $\text{RES}_e = \mathcal{O}(h^2)$  for all edges  $e$ .*

*Proof.* We will show begin with edge  $v_9$  which is sufficient.

$$\text{RES}_{v_9} = ikh^2 \mu_0^2 \nu \cos \theta \frac{\beta_1}{\beta_2} + \mathcal{O}(h^2) \quad (4.16)$$

$$\beta_1 = \epsilon_0 \mu_0 \left( 8\sqrt{\epsilon_0 \mu_0} - c_0^4 \left( 8\sqrt{\epsilon_0 \mu_0} (1 + 2q_5) + \epsilon_0 \mu_0 (1 - 16q_5) \right) \right) \quad (4.17)$$

$$- 8\sqrt{\epsilon_0 \mu_0} (\epsilon_0 \mu_0 - 1) \left( c_0^4 (1 + 2q_5) - 1 \right) \cot^2 \theta \quad (4.18)$$

$$+ 8c_0^2 \nu q_5 \cos \theta \left( \sqrt{\epsilon_0 \mu_0^3} (\epsilon_0 \mu_0 - 1) \cot^2 \theta + \epsilon_0 \mu_0 \left( (\epsilon_0 \mu_0 - 1) \cot^2 \theta \sqrt{\epsilon_0 \mu_0^3} \right. \right. \quad (4.19)$$

$$\left. \left. + \epsilon_0 \mu_0 \left( \sqrt{\epsilon_0 \mu_0^3} + \sqrt{1 + \epsilon_0^{-1} \mu_0^{-1} \cot^2 \theta} \right) \right) \right) \quad (4.20)$$

$$+ \epsilon_0 \mu_0 (8 + c_0^4 \left( \epsilon_0 \mu_0 \cot^2 \theta (16q_5 - 1) \sqrt{\epsilon_0 \mu_0^3} - 8(1 + 2q_5) \right) \left( 1 + \sqrt{\epsilon_0 \mu_0^3} \sqrt{1 + (1 - \epsilon_0^{-1} \mu_0^{-1}) \cot^2 \theta} \right) \quad (4.21)$$

$$\beta_2 = 4c_0^2 \sqrt{\epsilon_0 \mu_0^3} \left( 1 + \sqrt{\epsilon_0 \mu_0^3} \sqrt{1 + (1 - \epsilon_0^{-1} \mu_0^{-1}) \cot^2 \theta} \right)^2 \quad (4.22)$$

This rather complicated residual cannot be reduced to something  $\mathcal{O}(h^2)$  without selecting  $q_4$  dependent on wave parameters ( $k$  and  $\theta$ ). In order to correct for this introduced a convolution operator which would average nearby edges at time step  $n + 1$  to attempt to cancel additional errors. For example

$$v_9^{n+1} = \left( 1 - \gamma_1 + \gamma_2 (\exp(ikh \cos \theta) - 1) + \gamma_3 (\exp(-ikh \cos \theta) - 1) \right) \mathbf{E}_h^{n+1}|_{v_9} + \gamma_1 \mathbf{E}_h^{n+1}|_{v_4}. \quad (4.23)$$

Here the  $\gamma_2, \gamma_3$  are contributions from vertical edges to the left and right of  $v_9$ . Symmetry of these parameters is critical a method which will work for all possible angles. This therefore would produce a contribution of  $\gamma_2(\cos(kh \cos \theta) - 1)$  which will be of order  $\mathcal{O}(h^2)$  and therefore unable to cancel the lowest order errors present in the residual. We will therefore set  $\gamma_2 = \gamma_3 = 0$ .

The  $\gamma_1$  term seems more promising. However investigating the new residual with this term added presented difficulties. Call the new residual  $\text{RES}_{v_9}$ .

$$\widetilde{\text{RES}}_{v_9} = p(\epsilon_0, \mu_0, c_0, \gamma_1, q_5, k, \theta) + \sqrt{\frac{1 - 2\epsilon_0 \mu_0 + \cos 2\theta}{-\epsilon_0 \mu_0 + \epsilon_0 \mu_0 \cos 2\theta}} g(\epsilon_0, \mu_0, c_0, \gamma_1, q_5, k, \theta) + \mathcal{O}(h^2) \quad (4.24)$$

In this formulation we had  $p$  and  $g$  with no internal dependence on the square root term appearing in the expansion. This suggested that the only hope of eliminating one term was to eliminate the other and hope that  $g = p$ . However, the it is impossible to force  $g = 0$ . This can be shown by substituting the variable  $x = \exp(i\theta)$ .  $g$  can then be expanded in Dirichlet series from  $x^{-4}$  to  $x^4$ . With this in place it can be shown that the term is zero only if the coefficients for each term are identically zero. However, the over-determined system has no solution.

**Q.E.D.**

This leads to our first result, which is unfortunately negative. While the technique of applying both M-adaptation and convolution (averaging) provably does not work there is another option. To this end we will now focus on increasing accuracy at the interface by increasing the order of local polynomial

approximation. We will then have the layer adjacent to the interface with polynomial order 1 (as opposed to the lowest order which is only zero). The next layer out will now have hanging degrees of freedom associated with this higher refinement and we will apply M-adaptation to this to reduce dispersion over the non-physical interface the local increase in order will create.

## 5 Conclusions

In this work we attempted to extend previously successful m-adaptation ideas for Mimetic Finite Difference (MFD) discretizations of electric wave equation from homogeneous regions partitioned using uniform rectangular mesh to a flat interface problem with a factor of two wave speed difference. Our analysis showed that even in such ideal conditions of a flat interface and a factor of two mesh refinement this extension is not possible.

Our understanding of the reasons behind inability to successfully perform m-adaptation at the interface are the following. Even though MFD discretization, just like Yee scheme, is second order accurate on rectangular mesh this accuracy is achieved due to mesh symmetry. The same MFD scheme on unstructured mesh is only first order accurate. A factor of two refinement at the interface breaks mesh symmetry, therefore, defaulting the scheme to first order of accuracy at the interface. M-adaptation in homogeneous region effectively balanced the errors in spatial and temporal discretization, both of which were of second order. At the interface this balance is no longer possible as these errors are now of different order.

We also attempted a convolution approach, where we applied an additional averaging operator along the interface. Here the hope was that the first order error, being of odd order could be eliminated. Yet, this did not allow us to eliminate the error for all forms of incident waves, only for a particular ones, which is not sufficient for time domain formulations.

Our current vision of the discretization necessary for the interface problem is as follows. We need to encapsulate the interface and the parts of the homogeneous domains in a thin not necessarily structured mesh. Use a higher order implicit scheme on this mesh and couple it on both sides with the explicit solver. The advantages of this approach is that *(i)* it allows to deal with general interfaces (not necessarily flat ones); *(ii)* any jump in wave speed could be treated the same way; *(iii)* there are no restrictions on the time step (i.e. CFL condition) other than thickness of the interface layer due to implicit form of the method.

## 6 Acknowledgements

The work of Duncan McGregor was funded by Defense Thread Reduction Agency (DTRA) of the US Department of Defense grant DTRA10027-14741A1.

## References

- [1] W. S. Smith, A. Razmadze, X.-M. Shao, and J. L. Drewniak, “A hierarchy of explicit low-dispersion FDTD methods for electrically large problems,” *IEEE Transactions on Antennas and Propagation*, vol. 60, no. 12, pp. 5787–5800, 2012.
- [2] B. Yue and M. Guddati, “Dispersion-reducing finite elements for transient acoustics,” *J. Acoust. Soc. Am.*, vol. 118, pp. 2132–2141, 2005.
- [3] J. M. Hyman and M. Shashkov, “Mimetic discretizations for maxwell’s equations,” *J. Comput. Phys.*, vol. 151, pp. 881–909, 1999.
- [4] L. Beirão da Veiga, K. Lipnikov, and G. Manzini, *The Mimetic Finite Difference Method for Elliptic Problems*. Springer, 2013.

- [5] V. Gyrya, K. Lipnikov, G. Manzini, and D. Svyatskiy, “M-adaptation in the mimetic finite difference method,” *Math. Models Methods Appl. Sci.*, vol. 24, pp. 1621–1663, 2014.
- [6] V. Gyrya and K. Lipnikov, “M-adaptation method for acoustic wave equation on square meshes,” *J. Comp. Acoustics*, vol. 20, no. 4, pp. 1250022:1–23, 2012.
- [7] V. Gyrya and K. Lipnikov, “M-adaptation method for acoustic wave equation on rectangular meshes,” in *Proceedings of ENUMATH 2011, the 9th European conference on numerical mathematics and advanced applications, Leicester, UK, September 5–9, 2011* (A. Cangiani, ed.), Numerical mathematics and advanced applications 2011, pp. 429–439, Springer, 2013.
- [8] V. A. Bokil, N. L. Gibson, V. Gyrya, and D. A. McGregor, “Dispersion reducing methods for edge discretizations of the electric vector wave equation,” *Journal of Computational Physics*, vol. 287, pp. 88–109, 2015.
- [9] J. D. Jackson, *Classical Electrodynamics*. JOHN WILEY & SONS, INC., 1999.
- [10] L. Beirao da Veiga, K. Lipnikov, and G. Manzini, *The Mimetic Finite Difference Method for Elliptic Problems*. Springer, 2014.
- [11] F. Brezzi, L. Lipnikov, and M. Shashkov, “Convergence of mimetic finite difference methods for diffusion problems on polyhedral meshes,” *SIAM J. Num. Anal*, vol. 43, pp. 1872–1896, 2005.